Wearable EMG Bridge–a Multiple-Gesture Reconstruction System Using Electrical Stimulation Controlled by the Volitional Surface Electromyogram of a Healthy Forearm

ZHENGYANG BI[1], **YUNLONG WANG**[1], **HAIPENG WANG**[2], **(Member, IEEE)**,
YUXUAN ZHOU[3], **CHENXI XIE**[1], **LISEN ZHU**[2], **HONGXING WANG**[4], **BILEI WANG**[4],
JIA HUANG[4], **XIAOYING LÜ**[1,5], **AND ZHIGONG WANG**[2,5], **(Senior Member, IEEE)**

[1]State Key Lab of Bioelectronics, Southeast University, Nanjing 210096, China
[2]Institute of RF- & OE-ICs, Southeast University, Nanjing 210096, China
[3]School of Biomedical Engineering and Informatics, Nanjing Medical University, Nanjing 210009, China
[4]Department of Rehabilitation Medicine, Zhongda Hospital, Nanjing 210096, China
[5]Co-innovation Center of Neuroregeneration, Nantong University, Nantong 226001, China

Corresponding authors: Xiaoying Lü (luxy@seu.edu.cn) and Zhigong Wang (zgwang@seu.edu.cn)

ABSTRACT In this study, a wearable prototype system was developed for multiple-gesture rehabilitation using electrical stimulation controlled by a volitional surface electromyography (sEMG) scan of a healthy forearm. The purpose of the prototype system is to reconstruct multiple gestures of a paralysed limb and to simplify the positioning of sEMG detection sites on a healthy forearm. A self-designed eight-channel sEMG detection armband was used to detect the sEMG signal distributions of the muscle groups in healthy forearms. Linear discriminant analysis (LDA) was used to classify the sEMG signal distributions corresponding to different gestures, and then the classification results were mapped to corresponding stimulation channels. The sEMG signal with the maximum root mean square (RMS) was used as the source of stimulus coding for each gesture. Our proposed mean absolute value (MAV)/number of slope sign changes (NSS) dual-coding (MNDC) algorithm was used to encode the sEMG signal into an electrical stimulus with a dynamic pulse width and frequency. The constant-current stimulation armband electrically stimulated multiple muscles in the affected forearm by means of a circuit designed with a time-division multiplexed stimulation channel. An experiment involving 6 able-bodied volunteers showed that when the detection armband was located near the middle of the forearm, the gesture classification accuracy was greater than 90%, and each active sEMG signal was high. Gesture bridge experiments, including grasping, wrist flexion, wrist extension and finger extension, were carried out among six hemiplegic subjects and between one able-bodied volunteer acting as a controller and each of six stroke patients as the controllee. Both sets of results show that the proposed system can reconstruct these four gestures in the controlled subject with a delay of at most 360 ms and with a correlation coefficient of > 0.72.

INDEX TERMS Electrical stimulation, linear discriminant analysis (LDA), multiple-gesture reconstruction, paralysis, surface electromyography (sEMG).

I. INTRODUCTION

Functional electrical stimulation (FES) is a neurorehabilitation technique that is frequently used to maintain and restore limb motor function in patients with stroke and spinal cord injury (SCI) [1], [2]. Enhancing patients' volitional control in FES is key to improving its efficacy [3], [4]. Surface electromyography (sEMG) is used to measure the initiation of motion in patients and the contraction strength and fatigue of muscles and thus is commonly used as a basis for control

The associate editor coordinating the review of this manuscript and approving it for publication was Yizhang Jiang.

in FES systems to increase patients' participation. Several sEMG-controlled FES systems have been proposed, such as EMG-triggered FES [5], [6], proportional EMG-controlled FES [7] and contralaterally controlled FES (CCFES) [8]. In these techniques, patients' volitional sEMG signals are employed to trigger or regulate the FES system to assist the affected limb's movement. According to the theory of Hebbian plastic connections [9], [10], sEMG-controlled FES can gradually improve the motor rehabilitation effect by strengthening the synchronous activation of the central and peripheral nervous systems over time.

Currently, the most commonly used type of FES in the clinic is based on a 'switch'; however, this approach lacks patient participation and thus results in an unsatisfactory curative effect [4], [11]. In addition, the stimulation intensity of a 'switch'-based FES system cannot be adjusted dynamically, and hence, 'switch'-based FES fails to sufficiently regulate the evoked strength of the affected limb. Although proportional EMG-controlled FES and CCFES systems allow the FES intensity to be adjusted in accordance with the sEMG amplitude or the joint angle recorded by a bending sensor, they can generate only a single motion at a time [3], [7]. By contrast, most functional tasks, especially those involving an upper limb, involve the complex spatiotemporal coordination of multiple muscles [11]. Therefore, the rehabilitation of single movements performed by single muscles is insufficient.

For the control of multiple degrees of freedom in CCFES, the main limitation lies in the difficulty of achieving accurate control of the affected limb. Although EMG signal classifiers [12]–[15] and sEMG detection arrays [16] have been widely studied, most of them are used to control multidegree-of-freedom robotic prosthetics for amputees or for interactions in virtual reality. Considering the above limitations, our research group has proposed a novel method called the electromyography bridge (EMGB). The main idea of the EMGB is that each target muscle of a paralysed limb has its own source muscle in a healthy controller limb. Therefore, in the EMGB, a self-designed algorithm called the MNDC algorithm is applied to encode the mean absolute value (MAV) and number of slope sign changes (NSS) of the sEMG signal into the pulse width and frequency, respectively, of the stimulation [17], thus dynamically modulating the evoked muscle strength in real time. Subsequently, our research group has combined the EMGB with linear discriminant analysis (LDA) for multiple-gesture reconstruction [18]. However, the method presented in [18] is time consuming because it requires four sEMG detectors that need to be attached carefully at four sEMG detection sites on the forearm to capture the activation of multiple active muscles. Moreover, the system designed in [18] is relatively bulky and not suitable for patients' daily use.

In this study, we developed a prototype system called a wearable EMGB for multiple-gesture reconstruction on the affected side of the body. In the detection part of the system,

an eight-channel sEMG detection armband is used to detect the EMG distribution in a healthy forearm, and the channel with the strongest EMG amplitude is chosen as the detection site for each gesture. This method not only can ensure the accuracy of LDA but also can simplify the positioning of the detection sites. A time-division multiplexed (TDM) design is used for the stimulator to achieve multi-channel electrical stimulation. The MNDC algorithm is also adopted to realize accurate electrical stimulation control. In a preliminary clinical study, the ability of the prototype system to reconstruct hemiplegic patients' gestures based on the movements of an able-bodied person's hand has been tested. After a patient has participated in several training sessions and mastered the use of the detection armband, the CCFES paradigm, using the healthy side to control the affected side, can be implemented in combination with the proposed wearable EMGB.

The objectives of the current study were, first, to develop a wearable EMGB based on an ARM Core micro-controller and carry out a test with able-bodied volunteers and a clinical test to verify the feasibility of using the wearable EMGB for real-time gesture reconstruction and, second, to simplify the positioning of the sEMG detection sites while ensuring the sEMG-based gesture classification accuracy.

II. METHOD
A. EMGB OVERVIEW
The main idea of the EMGB is that each target muscle in a paralysed limb has its own source muscle in a healthy controller limb [19]. During the voluntary contraction of healthy muscles, the time-frequency characteristics of an sEMG scan of the healthy muscles can be encoded into a corresponding electrical stimulus, which can then be used to stimulate the corresponding affected muscles. As a result, the activation state of each healthy source muscle can be simulated in the paralysed limb in real time.

As shown in the block diagram of the system presented in Fig. 1, the wearable EMGB consists of an eight-channel sEMG detection armband and a four-channel constant-current stimulation armband. The sEMG detection armband consists of a micro-controller unit (MCU) for sEMG signal processing and a Bluetooth module for signal transmission. The stimulation armband consists of a Bluetooth receiving module, an MCU for stimulation regulation and a constant-current stimulation circuit. On the healthy forearm, the sEMG detection armband digitizes the sEMG signals, classifies the sEMG distribution via LDA and maps the classification results to the corresponding stimulation channels, locates the active sEMG signals and encodes them into stimulation parameters, and finally sends the stimulation channel numbers and stimulation parameters to the stimulation armband via Bluetooth. Based on the stimulation channel numbers and stimulation parameters, the stimulation armband activates the corresponding stimulation channels and then generates the desired electrical stimuli.
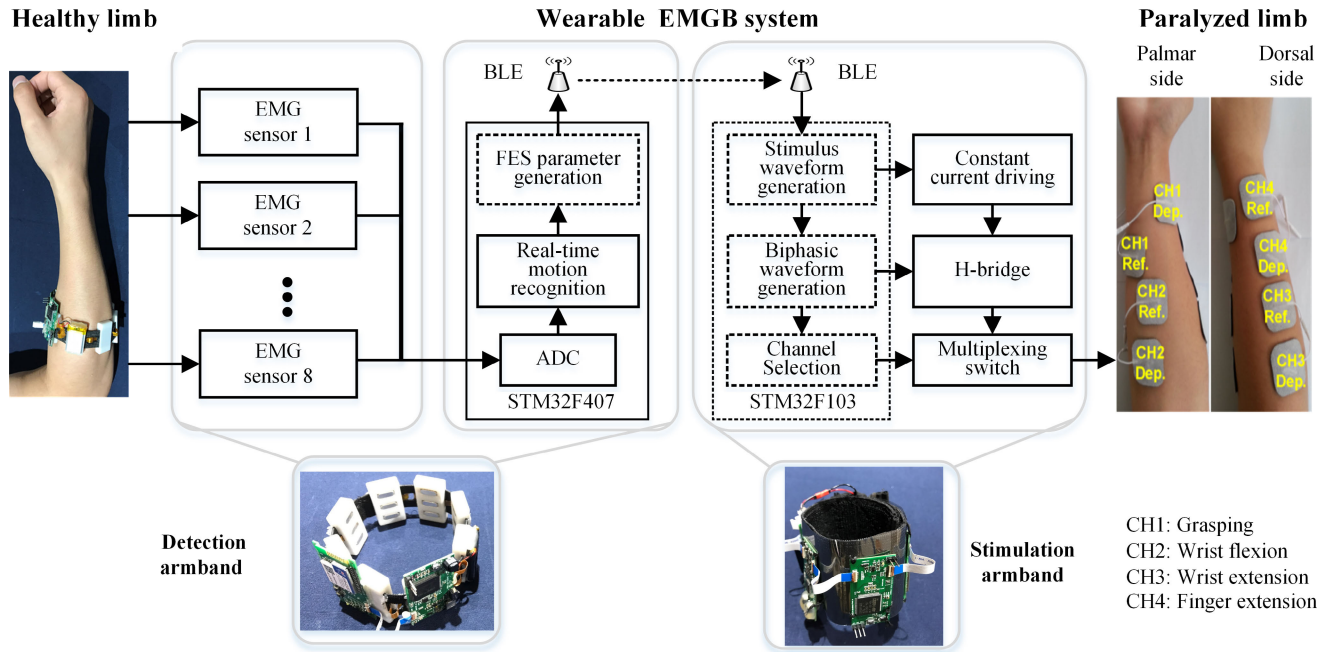
FIGURE 1. Block diagram of the wearable EMGB prototype and photographs of the detection armband and the stimulation armband.

B. HARDWARE DESIGN

In the detection armband, three dry silver electrodes are adopted for each sEMG detector for reusability. All eight common-ground sEMG detectors have a double differential configuration and a right leg driving circuit [19]. The passbands of the sEMG detectors range from 20 Hz to 450 Hz with a gain of 61 dB, and the voltage range of the output signals is 0 to 3.3 V. A flat cable is adopted to connect the eight sEMG detectors in a circle. A rubber band and eight resin shells are used to form the eight sEMG detectors into an armband with suitable tightness. As the MCU of the detection armband we use an STM32F407 micro-controller (STMicro-electronics, Inc., ITA&FR) because of its integrated digital signal processing (DSP) instruction and floating-point operation unit, which enhances the real-time performance of LDA. The sampling frequency is 1 kHz. A USR-BLE101 Bluetooth module (Youren Networking Technology Co., Ltd., China) is used to wirelessly transmit the stimulation parameters and stimulation channel numbers. The detection armband is powered by a 3.7-V, 380-mAh, 3.7-cm $\times$ 1.8-cm $\times$ 0.6-cm lithium battery.

In the stimulation armband, a USR-BLE101 Bluetooth module is employed to receive messages from the detection armband. As the MCU of the stimulation armband, we adopt an STM32F103 micro-controller (STMicroelec-tronics, Inc., ITA&FR) to modulate the electrical stimulation and activate/deactivate the stimulation channels. In the constant-current stimulator, an analogue switch chip is adopted to achieve a TDM design for the realization of four-channel electrical stimulation [20]. The maximum

output current of the stimulator is 30 mA, and the output voltage ranges from -60 V to 60 V.

To rapidly discharge the stimulation electrodes and thus reduce the influence of stimulation artefacts in the CCFES paradigm, the output stage of each stimulation channel is equipped with a MAX14803 analogue switch (Maxim Integrated Inc., USA) to short the stimulation electrodes after each stimulation. As the stimulation waveform, charge-balanced bi-directional asymmetric pulses are adopted to decrease muscle fatigue [21]. The 4 pairs of stimulation electrodes consist of 8 hydrogel electrodes attached to stimulation sites associated with grasping, wrist flexion, wrist extension and finger extension, corresponding to the first, second, third and fourth stimulation channels, respectively. The stimulation armband is powered by a 12-V, 1000-mAh, 5.1-cm $\times$ 1.5-cm $\times$ 1.5-cm lithium battery.

C. POSITIONING ANALYSIS OF THE DETECTION ARMBAND

For gesture reconstruction using the EMGB, the positioning of the detection sites is critical because the sEMG signals in the EMGB are used not only for gesture classification but also for stimulation encoding. For multiple-gesture reconstruction, the positioning process becomes much more time consuming due to the increase in the number of detection sites. In this study, we propose an eight-channel detection armband that surrounds the forearm, and we select the channel with the largest root mean square (RMS) signal for each gesture as the detection site to simplify the positioning of the detection sites. However, to ensure the accuracy of gesture
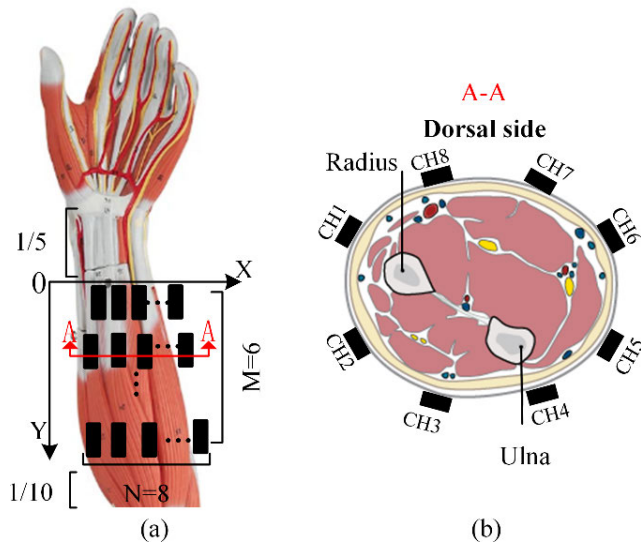
FIGURE 2. EMG detector distribution in the detection armband. (a) Top view of the distribution of the EMG detectors on the forearm. (b) Cross section of the 8 EMG detectors evenly distributed on the bisectrix at A-A.

classification while obtaining the strongest sEMG signals, a suitable reference position for the detection armband needs to be determined.

In this study, the detection sites for grasping, finger extension, wrist flexion and wrist extension, which are common targets of training in gesture rehabilitation, were investigated [3], [5], [11]. As shown in Fig. 2, to determine the reference position of the detection armband, the forearm was first divided into 5 equal parts from the distal 1 / 5 to the proximal 1 / 10, and these bisectrices were numbered from 1 to 6 (distal to proximal). Second, the detection armband was placed around the first bisectrix, with the eight sEMG detectors uniformly distributed. The subjects were required to complete the training procedure for the wearable EMGB (described in section II-D) with moderate force to generate an LDA model. Then, the LDA model was tested as the subjects successfully performed grasping, finger extension, wrist flexion and wrist extension four times. Each gesture was maintained for 4 s, with an interval of 2 s. Thus, the sEMG signal distribution and classification accuracy for a single bisectrix were obtained. The detection armband was then moved to the next bisectrix. This process was repeated until the sEMG signal distributions had been acquired and the classification accuracies determined for the whole forearm. Six able-bodied volunteers participated in this detection armband positioning analysis.

The RMS was calculated to represent the sEMG intensity, as shown in the following formula:

$$RMS = \sqrt{\frac{\sum_{i=1}^{N}(x_i - x_B)^2}{N}}, |x_i - x_B| > N_{\text{thr}} \quad (1)$$

Here, N_{thr} is 1.5 times the standard deviation (SD) of a 1 s data sample of background noise and x_B is the average of the

same data sample of background noise. Four RMS maps were drawn, corresponding to the sEMG signal distributions associated with the four gestures, and for each gesture, the region with the largest RMS was chosen as the detection site. The four RMS maps were normalized and were then multiplied by the maximum normalized RMS on the same bisectrix among all four maps to obtain the RMS products. The larger the RMS product is, the more balanced the bisectrix is among the four gestures. Finally, the classification accuracy and the RMS product for each bisectrix were combined to determine the best bisectrix, that is, the reference position for the detection armband.

D. ALGORITHMS FOR GESTURE CLASSIFICATION AND STIMULATION GENERATION

Compared with the artificial neural network (ANN) and support vector machine (SVM) algorithms, LDA achieves a similar classification accuracy and is less computationally expensive for small datasets; thus, it is more suitable for our study [13], [22]. Hudgins time-domain features, such as the MAV, number of zero crossings (NZC), NSS and wave length (WL), are usually used in sEMG-based motion classification because of their simplicity of computation and high classification accuracy [23], [24]. For these reasons, LDA and Hudgins time-domain features were adopted in our study.

The length of a data window was 150 ms, and the data windows of all eight channels were defined as an analysis frame. The step of the analysis frame was 50 ms. To reduce the computational resources consumed, it was necessary to determine whether each analysis frame contained sEMG before performing feature calculations and classification.

The WL features in the eight detection channels were used as a reference for analysing whether a frame contained an sEMG signal. Once a WL feature in any channel in an analysis frame exceeded the corresponding pre-set WL threshold, this analysis frame was identified as a motion frame. The WL threshold for each channel was set as follows: First, the average WL and WL SD of 200 consecutive analysis frames containing background noise were calculated. Then, the WL threshold for the channel was set to the sum of the average WL and 3 times the WL SD. The LDA model was trained on 320 motion frames of grasping, finger extension, wrist flexion and wrist extension (80 motion frames each). The possible classification results were grasping, wrist flexion, wrist extension, finger extension and no gesture, corresponding to channels 1, 2, 3, and 4 of the stimulator and no stimulation, respectively. To improve the gesture reconstruction accuracy, a classification result was sent only when three consistent results were consecutively generated.

Our MAV/NSS dual-coding (MNDC) algorithm was used to encode the MAV and NSS of an sEMG signal into the width and frequency, respectively, of the corresponding electrical stimulus to simulate autonomous forces [17]. The sEMG signal with the maximum RMS in each gesture frame was chosen as the coding source for the electrical stimulus. To improve
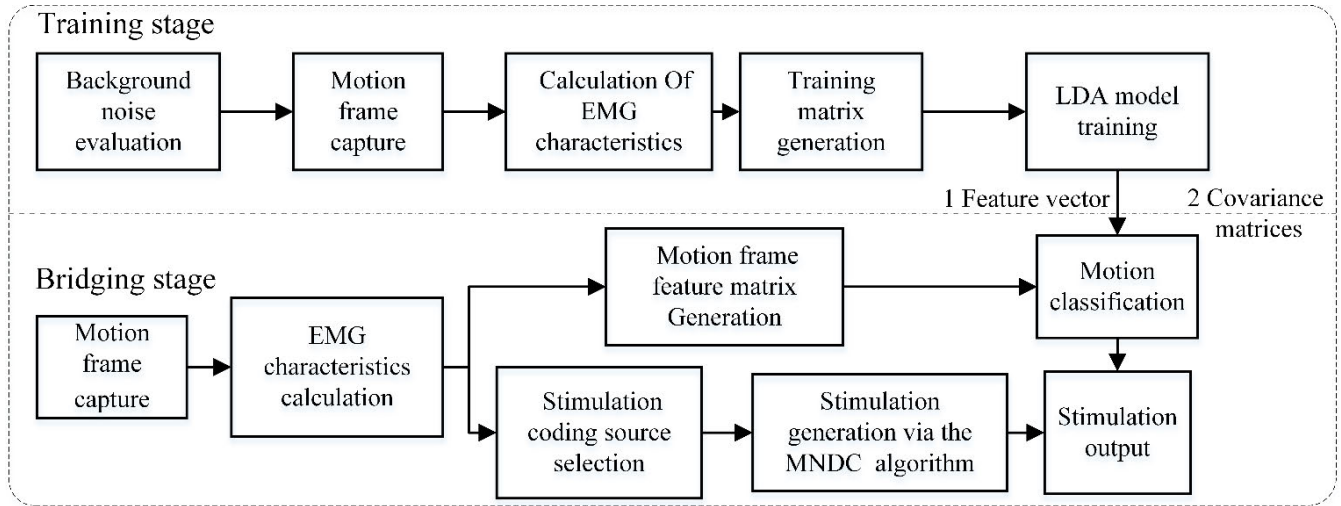
FIGURE 3. Flow chart of the training and bridging stages for the EMGB system.

the universality of the MNDC algorithm, the MAV and NSS of the sEMG signal need to be normalized individually before encoding. The generalized MNDC algorithm for wrist extension is shown in (2) and (3).

$$N_{pw} = 1.09 N_{\mathrm{MAV}} \qquad (2)$$
$$N_f = 1.09 N_{\mathrm{NSS}} \qquad (3)$$

The generalized MNDC algorithm for wrist flexion is given in (4) and (5).

$$N_{pw} = 0.82 N_{\mathrm{MAV}} \qquad (4)$$
$$N_f = 1.09 N_{\mathrm{NSS}} \qquad (5)$$

N_{pw} and N_f are the normalized stimulus pulse width and frequency, respectively, and N_{MAV} and N_{NSS} are the normalized *MAV* and *NSS* of the sEMG signal, respectively. The coefficients for grasping and finger extension were simply set to 1. The ranges of the stimulus pulse width and stimulus frequency were 200–700 μs and 20–60 Hz, respectively.

As shown in Fig. 3, the gesture reconstruction process in the wearable EMGB system consists of two stages: a training stage and a bridging stage. For the training stage, the subjects were asked to relax, and when a gesture was successfully completed, this was interactively indicated by LED indicators on the wearable EMG device. Finally, the WL thresholds for the eight channels and the trained LDA model parameters were obtained and stored in the RAM of the STM32F407 MCU. In the bridging stage, once a gesture frame was captured, the sEMG signal of this gesture frame was classified by the LDA model obtained in the training stage, and the classification result was mapped to a stimulation channel. At the same time, of the eight detection channels, the channel with the maximum RMS was chosen to encode the electrical stimulus. Finally, the stimulator output the stimulus to the corresponding stimulation channel.

E. EXPERIMENTAL PROTOCOLS
This study was approved by the Institutional Ethics Committee (IEC) for Clinical Research of ZhongDa Hospital, which is affiliated with Southeast University (Nanjing, China). The participants were recruited from the inpatient stroke rehabilitation programme at ZhongDa Hospital. Six able-bodied, right-handed volunteers (1 female and 5 male) aged 23 to 29 years and six stroke patients (2 females and 4 males) aged 44 to 70 years participated in this study. All subjects were asked to refrain from intense upper limb movement for at least 48 hours before the study, and each participant signed an informed consent form. The experimental scheme consists of two parts: part one was the positioning analysis of the detection armband, and part two was the real-time bridging test. The 6 able-bodied volunteers participated in both parts, and the 6 stroke patients and one able-bodied volunteer participated in part two.

1) POSITIONING ANALYSIS OF THE DETECTION ARMBAND
Each of the 6 able-bodied volunteers wore the detection armband on his or her right forearm, ensuring that the eight detection electrodes were in close contact with the skin. The subjects were asked to complete the processes described in section II-C to obtain the sEMG intensity distributions and the classification accuracies for the whole forearm. Finally, the RMS map and classification accuracy for each bisectrix were compared, the bisectrix with the largest RMS product was identified, and the general reference location for the detection armband was summarized. MATLAB R2015 was used to visualize the RMS maps of sEMG intensity. The PC used for the analysis had a 2.3 GHz Intel CPU and 4 GB of memory.

2) BRIDGING TEST
In the bridging test, the 6 able-bodied volunteers were randomly divided into three groups, with two volunteers in each group. One volunteer wore the detection armband on his or

her right forearm and acted as the controller, and the other volunteer wore the stimulation armband on his or her right forearm and acted as the controllee. After each experiment, the participants switched roles, and the test was repeated. In total, 6 functional reconstruction experiments were conducted. To avoid cheating, the volunteer acting as the controllee wore a blindfold and was asked to avoid active motion. In the clinical trials, each stroke patient wore the stimulation armband on the affected side, and the able-bodied volunteer wore the detection armband and acted as the controller. The patients were encouraged to imagine performing the corresponding gestures during reconstruction.

In the bridging test with the able-bodied volunteers, the subject acting as the controller was required to alternately perform wrist extension and wrist flexion 8 times each and then alternately perform finger extension and grasping 8 times each. The angles of the hand joints of the controller and controllee were tracked using a Leap Motion sensor (Leap Ltd., San Francisco). In this experiment, the knuckle angle was defined as the average metacarpophalangeal joint angle (D_{MPJ}) of the four fingers, excluding the thumb, and the wrist joint angle (D_{WJ}) was defined as the angle between the palm and the forearm. The neutral position in the effective gesture range of the two angles was set to 0°. The cross-correlation of the normalized D_{MPJ} and D_{WJ} of each participant were then calculated as formula (6).

$$\rho_{xy}^2(m) = \frac{\left(\sum x(n)y(n+m)\right)^2}{\sum x^2(n)\sum y^2(n)} \tag{6}$$

where $x(n)$ and $y(n)$ are the joint angle trajectories of the controller and controllee, respectively, and m is a variable related to the delay time (T_d). Thus, the correlation and synchronization between the joint angles of the controlling and controlled limbs could be obtained.

The subject acting as the controller then performed the four gestures 80 times with voluntary variations in duration; the four gestures were performed in a random order, with an even distribution of the number of times each gesture was performed, in accordance with a random table. A reconstruction was considered successful if the controlled hand produced the same gesture as that performed by the controlling hand within 0.5 s. Then, the success rate (R_s) for each of the four gestures was calculated.

In the clinical experiment, the controlled subject was required to perform each of the four gestures 20 times, separated into four groups. Each group contained only one kind of gesture. The correlation and synchronization between the joint angles of the controlled and controlling limbs were calculated from the reconstruction data corresponding to the first 8 repetitions of each movement, and the success rate of the reconstruction of each movement was calculated from the overall data. The 0° positions of the finger joint and wrist joint, the recording device, the cross-correlation calculation method, and the judgement of successful reconstruction were the same as they were in the bridging test with the able-bodied volunteers.
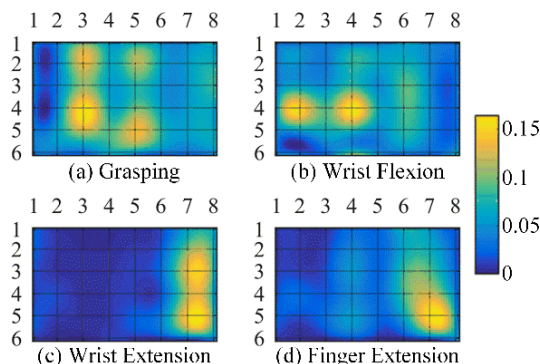

FIGURE 4. sEMG RMS maps of subject A recorded during the four gestures: (a) grasping, (b) wrist flexion, (c) finger extension, and (d) wrist extension.

TABLE 1. Motion classification accuracy (CA), macro F1, kappa statistics and the number of times associated with the RMS product peak for each bisectrix.

Bisectrix	CA (%)	Macro F1	Kappa Statistics	Number of RMS product peaks
1	89.99 ± 8.84	0.90	0.87	0
2	88.28 ± 1.76	0.88	0.84	1
3	94.21 ± 2.22*	0.94	0.92	2
4	93.23 ± 1.86*	0.93	0.90	3
5	92.45 ± 2.26*	0.92	0.86	0
6	89.44 ± 4.26	0.89	0.82	0

F. STATISTICAL ANALYSIS

To assess whether the location of the detection armband had a significant effect on the motion classification accuracy, a one-way analysis of variance (ANOVA) (among the 6 bisectrices) was performed on the classification accuracy results. Pairwise comparison with Bonferroni correction was performed if a significant main effect was observed. Differences with $P < 0.05$ were considered significant.

A t-test was performed to assess the R_s differences between the bridging results from the able-bodied volunteers and the clinical experiment. Pairwise comparison with Bonferroni correction was performed if a significant main effect was observed. Differences with $P < 0.001$ were considered significant.

The statistical analyses were performed using SPSS Statistics 19.0.

III. RESULTS
A. POSITIONING ANALYSIS OF THE DETECTION ARMBAND

Fig. 4 shows subject A's RMS maps recorded during the four gestures after cubic spline interpolation. In relation to human anatomy, the yellow areas shown in Fig. 4 (a), Fig. 4 (b), Fig. 4 (c) and Fig. 4 (d), correspond to the flexor digitorum superficialis, the flexor carpi radialis and flexor carpi ulnaris, the extensor carpi ulnaris, and the extensor digitorum, respectively.
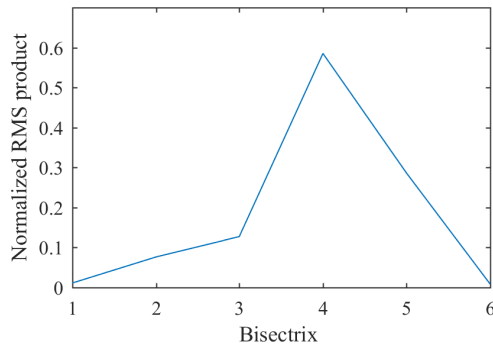
FIGURE 5. RMS product distribution of subject A.

FIGURE 6. Confusion matrix for each bisectrix. TL: true label, PL: predicted label, GP: grasping, WF: wrist flexion, FE: finger extension, WE: wrist extension.
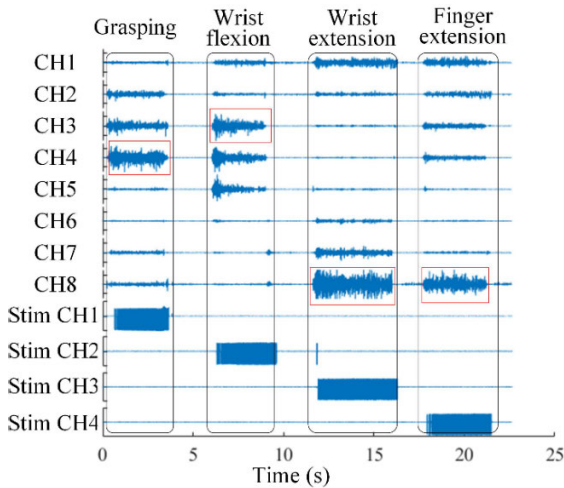

FIGURE 7. Stimulus generation results from the real-time bridging test for subject A. The EMG signals in the red solid boxes are the stimulus coding sources corresponding to the respective stimulus channels.

Fig. 5 shows subject A's RMS product distribution, which peaks at the fourth bisectrix. The classification accuracy (CA) values for the four gestures on different bisectrices and the number of times each bisectrix associated with the maximum RMS product are illustrated in Table 1. The one-way ANOVA
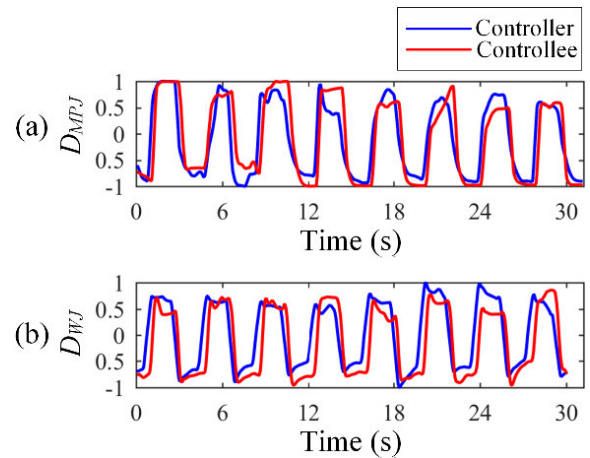

FIGURE 8. Bridging test results for controller A and controllee B: (a) the trajectories of D_{MPJ} and (b) the trajectories of D_{WJ}. The blue and red lines correspond to controller A and controllee B, respectively.

results comparing the CAs for each bisectrix show that the CAs for the third, fourth and fifth bisectrices are significantly higher than those for the other bisectrices (*$P < 0.05$). The macro F1 for each bisectrix is greater than 0.88 and reveals that a classification with high recall and precsion has been achieved. The kappa statistics for each bisectrix is greater than 0.82 and indicates the high consistency of the classification.

Fig. 6 shows the confusion matrices of the CA for each gesture with the detection armband at each bisectrix. The confusion matrices indicate the same results: the third, fourth and fifth bisectrices yield higher CAs than the other bisectrices, as in Table 1.

B. BRIDGING TEST

Fig. 7 shows representative stimulus generation results from the real-time bridging test. For each gesture, the channel in the red box has the maximum RMS and is therefore selected as the stimulus coding source.

Fig. 8 show the normalized D_{WJ} and D_{MPJ} trajectories of subjects A and B in the bridging test involving the healthy volunteers. As seen from Table 2, the mean maximum correlation coefficients of D_{WJ} and D_{MPJ} between the controller and controllee in the bridging test with the able-bodied volunteers were 0.84 ± 0.04 and 0.87 ± 0.03, respectively. These results indicate that the wearable EMGB can be successfully used to reproduce desired gestures in a controlled hand.

Fig. 9 depicts the maximum correlations in D_{WJ} and D_{MPJ} and the corresponding delays from Fig. 8. The mean delays in D_{WJ} and D_{MPJ} between the control hand and the controlled hand were approximately 270 ± 62.2 ms and 305 ± 33.9 ms, respectively, which satisfy the time-delay requirements for real-time neural prosthesis control [25].

As seen from Table 3, the mean R_s values from the 6 randomized controlled trials of grasping, finger extension, wrist

TABLE 2. Maximum correlations and delays in the bridging test with able-bodied volunteers.

	Max (ρ_{xy}) (D_{WJ})	T_d (ms) (D_{WJ})	Max (ρ_{xy}) (D_{MPJ})	T_d (ms) (D_{MPJ})
A-B	0.92	270	0.93	290
B-A	0.79	230	0.89	320
C-D	0.83	330	0.88	300
D-C	0.88	360	0.82	250
E-F	0.85	220	0.86	350
F-E	0.82	210	0.89	320

TABLE 3. R_S results from the randomized motion control test with able-bodied volunteers.

	R_s (%) GP [a]	R_s (%) FE [a]	R_s (%) WF [a]	R_s (%) WE [a]
A-B	90	90	90	95
B-A	95	85	95	95
C-D	85	90	90	95
D-C	85	95	95	95
E-F	95	85	90	90
F-E	90	90	95	95

[a]GP: grasping, FE: finger extension, WF: wrist flexion WE: wrist extension.

TABLE 4. Maximum correlations, delays and R_S values for grasping (GP) and finger extension (FE) in the bridging test involving stroke patients.

	GP Max (ρ_{xy})	GP T_d (ms)	GP R_s (%)	FE Max (ρ_{xy})	FE T_d (ms)	FE R_s (%)
1	-	-	-	0.92	260	80
2	0.88	300	75	0.81	270	85
3	0.84	280	85	0.76	320	90
4	0.88	310	80	0.83	350	75
5	0.84	460	50	0.79	270	55
6	0.72	480	30	0.82	290	60

TABLE 5. Maximum correlations, delays and R_S values for wrist flexion (WF) and wrist extension (WE) in the bridging test involving stroke patients.

	WF Max (ρ_{xy})	WF T_d (ms)	WF R_s (%)	WE Max (ρ_{xy})	WE T_d (ms)	WE R_s (%)
1	0.86	290	95	290	270	90
2	0.90	300	90	320	230	95
3	0.92	300	90	300	330	95
4	0.96	290	95	250	360	90
5	0.83	320	90	350	280	95
6	0.89	350	85	320	310	95
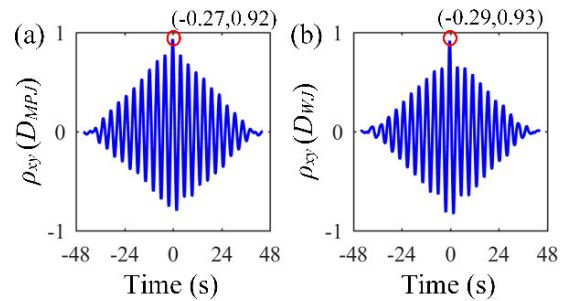
FIGURE 9. Maximum correlations and corresponding delays between controller A and controllee B: (a) the correlation and synchronization of D_{MPJ} and (b) the correlation and synchronization of D_{WJ}. In each panel, the red circle indicates the maximum correlation and the corresponding delay.

As shown in Fig. 12, pairwise comparisons using Bonferroni adjustment revealed that, in the clinical trials, the bridging of wrist flexion and wrist extension resulting in significantly higher R_s values than the bridging of grasping and finger extension (***$P < 0.001$). In addition, in the bridging of grasping and finger extension, the R_s between able-bodied volunteers was much higher than that between an able-bodied volunteer and a stroke patient (***$P < 0.001$).

IV. DISCUSSION

First, this paper studied the effect of the position of the detection armband on the detected sEMG intensity and the gesture CA. The position analysis showed that wearing the detection armband near the third, fourth or fifth bisectrix of the forearm not only allows a strong sEMG signal to be detector for each of the four gestures but also ensures a high CA (> 90%).

As presented in Table 3, the real-time bridging test results for the able-bodied volunteers show the success rates for the reconstruction of the four gestures were all greater than 85%. In addition, in the clinical trials, the successful reconstruction of gestures in hemiplegic patients under the control of able-bodied volunteers indicates that the wearable EMGB can provide an effective means of gesture training. In addition, the bridging test results from both the test with the able-bodied volunteers and the clinical trials indicate that the delay time between the controlling limb and the controlled limb is approximately 300 ms, satisfying the requirements for a real-time neural prosthesis [1], [25]. However, there were also some unsuccessful cases in the randomized controlled
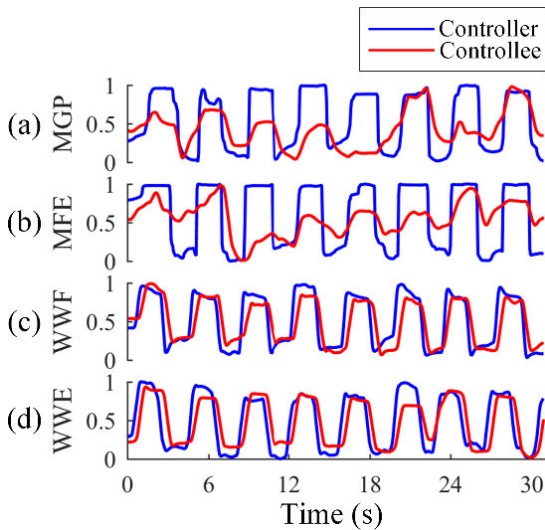
flexion and wrist extension were 90.0 ± 4.4%, 89.1 ± 3.7%, 92.5 ± 2.7%, and 94.1 ± 2.0%, respectively.

Fig. 10 shows the normalized D_{WJ} trajectories of grasping and finger extension and the normalized D_{MPJ} trajectories of wrist flexion and wrist extension for patient 4 in the clinical bridging test. Fig. 11 shows the maximum correlations in D_{WJ} and D_{MPJ} and the corresponding delays from Fig. 10.

As seen from Table 4 and Table 5, the mean maximum correlation coefficients of D_{WJ} or D_{MPJ} for grasping, finger extension, wrist flexion and wrist extension between the controller and the patient were 0.83 ± 0.05, 0.87 ± 0.02, 0.89 ± 0.05 and 0.89 ± 0.04, respectively. The mean delays in the reconstruction of grasping, finger extension, wrist flexion and wrist extension were 366 ± 95.8 ms, 296 ± 46.3 ms, 293 ± 35.0 ms, and 308 ± 23.1 ms, respectively. Patient I was unable to carry out the grasping bridging test due to discomfort with the electrical stimulation; thus, there are no grasping data for patient I. The mean R_s values in the 6 clinical trials of grasping, finger extension, wrist flexion and wrist extension were 64 ± 23.2%, 74.1 ± 13.9%, 90.8 ± 3.7% and 93.3 ± 2.5%, respectively.
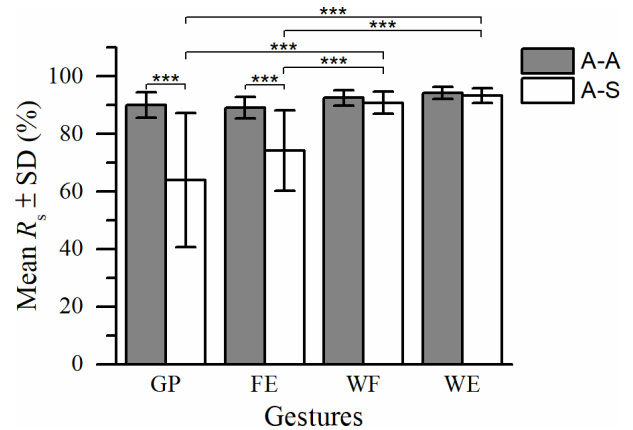
FIGURE 10. Bridging test results for an able-bodied person and stroke patient 4: (a) MGP, D_{MPJ} during grasping; (b) MFE, D_{MPJ} during finger extension; (c) WWF, D_{WJ} during wrist flexion; and (d): WWE, D_{WJ} during wrist extension. The blue and red lines correspond to the able-bodied person and stroke patient 4, respectively.
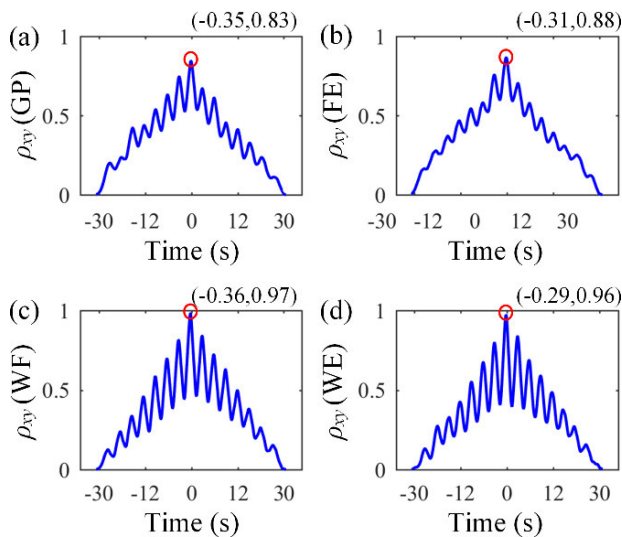
FIGURE 11. Maximum correlations and corresponding delays between the able-bodied person and stroke patient 4 during the four gestures: (a) the correlation and delay in D_{MPJ} during grasping(GP), (b) the correlation and delay in D_{MPJ} during finger extension(FE), (c) the correlation and delay in D_{WJ} during wrist flexion(WF), and (d) the correlation and delay in D_{WJ} during wrist extension(WE). In each panel, the red circle indicates the maximum correlation and the corresponding delay.

FIGURE 12. Mean R_s values from bridging tests with able-bodied volunteers (A-A) and with an able-bodied volunteer controlling a stroke patient (A-S). The results are shown as the mean $R_s \pm$ SD (%) (n = 6). ***$P < 0.001$, as determined by pairwise comparison using Bonferroni adjustment. GP: grasping, WF: wrist flexion, FE: finger extension, WE: wrist extension.

$64 \pm 23.2\%$, respectively, ***$P < 0.001$), as shown in Fig. 12, partly because the flexor carpi radialis and flexor carpi ulnaris are located on the dorsal and palmar surfaces of the forearm, respectively, and are easy to recruit through electrical stimuli. In addition, to achieve independent finger extension and grasping, stimulation electrodes are often attached to the front of the forearm to avoid recruiting the muscles responsible for wrist flexion and wrist extension, resulting in a relatively lower level of muscle recruitment for finger extension and grasping. Moreover, most stroke patients need a higher current intensity for stimulation than able-bodied volunteers do [27, 28], which accelerates muscle fatigue and further decreases the success rate of finger extension and grasping reconstruction. A comparison between the bridging results from the able-bodied subjects and the clinical trials shows that there are no significant differences in the mean success rates for wrist extension and wrist flexion ($92.5 \pm 2.7\%$ vs. $93.3 \pm 2.5\%$ and $94.1 \pm 2.0\%$ vs. $90.8 \pm 3.7\%$, respectively). The main reason is that all the selected patients had suffered a stroke within 3 months prior, and therefore, the muscle atrophy and motor unit alienation were moderate. However, the mean reconstruction success rates for finger extension and grasping were significantly higher in the able-bodied subjects than in the stroke patients ($90.0 \pm 4.4\%$ vs. $74.1 \pm 13.9\%$ and $89.1 \pm 3.7\%$ vs. $64 \pm 23.2\%$, ***$P < 0.001$, respectively). The main reason is partly the same as the reason for the accelerated process of muscle fatigue discussed above.

Table 6 illustrates the comparison between wearable EMGB and other gestures reconstruction systems. Cunningham David A. *et al.* [29] proposed a CCFES system to reconstruct wrist extension and wrist flexion of the affected hand of hemiplegic patients. This CCFES system employed a data glove to detect the gestures from the healthy hand and thus to trigger fixed electrical stimulation on the affected side. Dingguo Zhang *et al.* [30] proposed a CCFES system to enhance the gestures of the affected hand. In this system,

trials in the latter half of the bridging test with the able-bodied volunteers. This may have been due to muscle fatigue or characteristic changes in the skin-electrode interface during repetitive movements of the controlling or controlled limbs [12], [26], which also appeared in the clinical trials. In the clinical trials, the mean success rates for the reconstruction of wrist extension and wrist flexion ($93.3 \pm 2.5\%$ and $90.8 \pm 3.7\%$, respectively) were significantly higher than those for finger extension and grasping ($74.1 \pm 13.9\%$ and

TABLE 6. The Comparison between wearable EMGB and other gestures reconstruction systems.

	Cunningham, David A. et al. [29]	Dingguo Zhang et al. [30]	Wearable EMGB
Control method	Data glove	Four to nine channels sEMG	Eight channels sEMG
Gestures	Two (WE, WF) [a]	One (customized)	Four (customized)
Stimulation intensity	Fixed	Adjusted by sEMG from healthy arm	Adjusted by sEMG from healthy arm
Clinical validation	Yes	No	Yes

[a]WE: wrist extension, WF: wrist flexion

the stimulation intensity of each channel was pre-set according to the sEMG bias between the healthy forearm and the affected forearm during performing one customized gesture. However, the stimulation intensity could not be controlled by users during enhancing stage. Compared with these two CCFES systems, wearable EMGB can reconstruct four customized gestures and adjust the stimulation intensity volitionally.

In addition, the training procedure for the wearable EMGB may be difficult for stroke patients to perform. Although the healthy limb of a stroke patient is almost the same as that of an able-bodied person, the gestures of a stroke patient before and after the training stage are usually not consistent or independent. For instance, wrist flexion and wrist extension in stroke patients are always accompanied by finger extension, resulting in a low accuracy in the classification of gestures; consequently, more training guidance is required to improve the training effect.

The detection armband and the stimulation armband of wearable EMGB employ a wearable and wireless design to enable their use in the daily life of patients. The eight-channel detection armband greatly reduces the difficulty of detection site selection. In addition, beyond just the four hand movements studied here (grasping, finger extension, wrist extension, and wrist flexion), the wearable EMGB can also reconstruct even more subtle finger movements.

V. CONCLUSION

A wearable real-time controlled multi-channel EMGB has been proposed. The detection armband based on eight sEMG detectors greatly reduces the difficulty of detection site selection. LDA for gesture classification based on sEMG and a four-channel stimulation armband are used to realize the real-time control of an affected limb by a healthy limb. Bridging test results from both tests with able-bodied volunteers and clinical trials show that four hand movements performed on the controller side can be reconstructed with high accuracy and low delay on the controlled side. In the future, further study will be necessary on how to simplify the positioning of the stimulation sites to facilitate patients' daily use.

REFERENCES

[1] D. Koutsou, S. Summa, B. Nasser, J. G. Martinez, and M. Thangaramanujam, "Upper limb neuroprostheses: Recent advances and future directions," in *Emerging Therapies in Neurorehabilitation*. Berlin, Germany: Springer-Verlag, 2014, pp. 207–233.

[2] O. Schuhfried, R. Crevenna, V. Fialka-Moser, and T. Paternostro-Sluga, "Non-invasive neuromuscular electrical stimulation in patients with central nervous system lesions: An educational review," *J. Rehabil. Med.*, vol. 44, no. 2, pp. 99–105, Feb. 2012.

[3] J. S. Knutson, M. Y. Harley, T. Z. Hisel, S. D. Hogan, M. M. Maloney, and J. Chae, "Contralaterally controlled functional electrical stimulation for upper extremity hemiplegia: An early-phase randomized clinical trial in subacute stroke patients," *Neurorehabil. Neural Repair*, vol. 26, pp. 239–246, Mar./Apr. 2012.

[4] S. C. McGie, J. Zariffa, M. R. Popovic, and M. K. Nagai, "Short-term neuroplastic effects of brain-controlled and muscle-controlled electrical stimulation," *Neuromodulation, Technol. Neural Interface*, vol. 18, no. 3, pp. 233–240, Apr. 2015.

[5] J. Cauraugh, K. Light, S. Kim, M. Thigpen, and A. Behrman, "Chronic motor dysfunction after stroke: Recovering wrist and finger extension by electromyography-triggered neuromuscular stimulation," *Stroke*, vol. 31, pp. 1360–1364, Jun. 2000.

[6] H. K. Shin, S. H. Cho, H.-S. Jeon, Y.-H. Lee, J. C. Song, S. H. Jang, C.-H. Lee, and Y. H. Kwon, "Cortical effect and functional recovery by the electromyography-triggered neuromuscular stimulation in chronic stroke patients," *Neurosci. Lett.*, vol. 442, pp. 174–179, Sep. 2008.

[7] Y. Hara, S. Obayashi, K. Tsujiuchi, and Y. Muraoka, "The effects of electromyography-controlled functional electrical stimulation on upper extremity function and cortical perfusion in stroke patients," *Clin Neurophysiol.*, vol. 124, pp. 2008–2015, Oct. 2013.

[8] I. K. Niazi, N. Mrachacz-Kersting, K. Jiang, K. Dremstrup, and D. Farina, "Peripheral electrical stimulation triggered by self-paced detection of motor intention enhances motor evoked potentials," *IEEE Trans. Neural Syst. Rehabil. Eng.*, vol. 20, no. 4, pp. 595–604, Jul. 2012.

[9] C. Buetefisch, R. Heger, W. Schicks, R. Seitz, and J. Netz, "Hebbian-type stimulation during robot-assisted training in patients with stroke," *Neurorehabil. Neural Repair*, vol. 25, no. 7, pp. 645–655, Sep. 2011.

[10] B. B. Johansson, "Brain plasticity and stroke rehabilitation: The Willis lecture," *Stroke*, vol. 31, no. 1, pp. 223–230, Jan. 2000.

[11] B. C. Craven, S. C. Hadi, and M. R. Popovic, "Functional electrical stimulation therapy: Enabling function through reaching and grasping," in *International Handbook of Occupational Therapy Interventions*. Springer, 2015, pp. 587–605.

[12] N. Jiang, S. Dosen, K. R. Muller, and D. Farina, "Myoelectric control of artificial limbs—Is there a need to change focus? [In the spotlight]," *IEEE Signal Process. Mag.*, vol. 29, no. 5, pp. 147–150, Sep. 2012.

[13] L. J. Hargrove, K. Englehart, and B. Hudgins, "A comparison of surface and intramuscular myoelectric signal classification," *IEEE Trans. Biomed. Eng.*, vol. 54, no. 5, pp. 847–853, May 2007.

[14] A. Subasi and S. M. Qaisar, "Surface EMG signal classification using TQWT, bagging and boosting for hand movement recognition," *J. Ambient Intell. Hum. Comput.*, Apr. 2020, doi: 10.1007/s12652-020-01980-6.

[15] T. Tuncer, S. Dogan, and A. Subasi, "Surface EMG signal classification using ternary pattern and discrete wavelet transform based feature extraction for hand movement recognition," *Biomed. Signal Process. Control*, vol. 58, Apr. 2020, Art. no. 101872.

[16] T. R. Farrell and R. F. Weir, "A comparison of the effects of electrode implantation and targeting on pattern classification accuracy for prosthesis control," *IEEE Trans. Biomed. Eng.*, vol. 55, no. 9, pp. 2198–2211, Sep. 2008.

[17] Y. Zhou, Y. Xia, J. Huang, H. Wang, X. Bao, Z. Bi, X. Chen, Y. Gao, X. Lü, and Z. Wang, "Electromyographic bridge for promoting the recovery of hand movements in subacute stroke patients: A randomized controlled trial," *J. Rehabil. Med.*, vol. 49, no. 8, pp. 629–636, 2017.

[18] Y.-X. Zhou, H.-P. Wang, X.-P. Cao, Z.-Y. Bi, Y.-J. Gao, X.-B. Chen, X.-Y. Lu, and Z.-G. Wang, "Electromyographic Bridge—A multi-movement volitional control method for functional electrical stimulation:

Prototype system design and experimental validation," in *Proc. 39th Annu. Int. Conf. IEEE Eng. Med. Biol. Soc. (EMBC)*, Jul. 2017, pp. 205–208.

[19] Z. Wang, X. Lv, Y. Zhou, H. Wang, S. Zong, and Z. Huang, "A novel functional electrical stimulation-control system for restoring motor function of post-stroke hemiplegic patients," *Neural Regeneration Res.*, vol. 9, no. 23, p. 2102, 2014.

[20] H.-P. Wang, A.-W. Guo, Y.-X. Zhou, Y. Xia, J. Huang, C.-Y. Xu, Z.-H. Huang, X.-Y. Lü, and Z.-G. Wang, "A wireless wearable surface functional electrical stimulator," *Int. J. Electron.*, vol. 104, no. 9, pp. 1514–1526, 2017.

[21] D. R. Merrill, M. Bikson, and J. G. R. Jefferys, "Electrical stimulation of excitable tissue: Design of efficacious and safe protocols," *J. Neurosci. Methods*, vol. 141, no. 2, pp. 171–198, Feb. 2005.

[22] K. Englehart, B. Hudgins, P. A. Parker, and M. Stevenson, "Classification of the myoelectric signal using time-frequency based representations," *Med. Eng. Phys.*, vol. 21, nos. 6–7, pp. 431–438, Jul./Sep. 1999.

[23] Y. Huang, K. B. Englehart, B. Hudgins, and A. D. C. Chan, "A Gaussian mixture model based classification scheme for myoelectric control of powered upper limb prostheses," *IEEE Trans. Biomed. Eng.*, vol. 52, no. 11, pp. 1801–1811, Nov. 2005.

[24] B. Hudgins, P. Parker, and R. N. Scott, "A new strategy for multifunction myoelectric control," *IEEE Trans. Biomed. Eng.*, vol. 40, no. 1, pp. 82–94, Jan. 1993.

[25] K. Englehart and B. Hudgins, "A robust, real-time control scheme for multifunction myoelectric control," *IEEE Trans. Biomed. Eng.*, vol. 50, no. 7, pp. 848–854, Jul. 2003.

[26] D. Tkach, H. Huang, and T. A. Kuiken, "Study of stability of time-domain features for electromyographic pattern recognition," *J. Neuroeng. Rehabil.*, vol. 7, no. 1, p. 21, 2010.

[27] N. Scherbakov and W. Doehner, "Sarcopenia in stroke-facts and numbers on muscle loss accounting for disability after stroke," *J. Cachexia, Sarcopenia Muscle*, vol. 2, no. 1, pp. 5–8, Mar. 2011.

[28] C. English, H. McLennan, K. Thoirs, A. Coates, and J. Bernhardt, "Loss of skeletal muscle mass after stroke: A systematic review," *Int. J. Stroke*, vol. 5, no. 5, pp. 395–402, 2010.

[29] D. A. Cunningham, J. S. Knutson, V. Sankarasubramanian, K. A. Potter-Baker, A. G. Machado, and E. B. Plow, "Bilateral contralaterally controlled functional electrical stimulation reveals new insights into the interhemispheric competition model in chronic stroke," *Neurorehabil. Neural Repair*, vol. 33, no. 9, pp. 707–717, Sep. 2019.

[30] Y. Zhou, Y. Fang, K. Gui, K. Li, D. Zhang, and H. Liu, "SEMG bias-driven functional electrical stimulation system for upper-limb stroke rehabilitation," *IEEE Sensors J.*, vol. 18, no. 16, pp. 6812–6821, Aug. 2018.

ZHENGYANG BI received the B.S. degree in biomedical engineering from the Hefei University of Technology, Hefei, China, in 2013, and the M.S. degree in biomedical engineering from Southeast University, Nanjing, China, in 2016, where he is currently pursuing the Ph.D. degree in biomedical engineering. His current research interests include biomedical signal processing, neuroprosthesis system design, and rehabilitation engineering.

YUNLONG WANG received the B.S. degree in biomedical engineering and the M.S. degree in biomedical engineering from Southeast University, Nanjing, China, in 2016 and 2019, respectively. His current research interests include biomedical signal processing, neuroprosthesis system design, and rehabilitation engineering.

HAIPENG WANG (Member, IEEE) received the B.S. degree in electronic engineering from the Shandong University of Science and Technology, Qingdao, China, in 2009, the M.S. degree in electronic engineering from Xidian University, Xi'an, China, in 2012, and the Ph.D. degree in circuits and systems from the Institute of RF& OE-ICs, Southeast University, Nanjing, China, in 2017. From 2017 to 2019, he worked as a Lecturer at the School of Electronic and Information Engineering, Sanjiang University, Nanjing. Since September 2019, he has been working as a Postdoctoral Fellow with Southeast University. His research interests include biomedical circuit and system design, and biomedical signal processing.

YUXUAN ZHOU received the B.S. degree in mechanical engineering and automation from the Nanjing University of Science and Technology, Nanjing, China, in 2007, the M.S. degree in biomedical engineering from Nanjing Medical University, Nanjing, in 2010, and the Ph.D. degree in biomedical engineering from Southeast University, Nanjing, in 2019.

He is currently a Lecturer in biomedical engineering with Nanjing Medical University. His research interests include biomedical signal processing, neural rehabilitation systems, and flexible electronic devices.

CHENXI XIE received the B.S. degree in biomedical engineering from Southeast University, Nanjing, China, in 2018, where he is currently pursuing the M.S. degree in biomedical engineering. His research interests include electrical system design, rehabilitation engineering, and biomedical signal processing.

LISEN ZHU received the B.S. degree in measurement and control technology and instruments from the East China University of Science and Technology, Shanghai, China, in 2018. He is currently pursuing the M.S. degree in integrated circuit engineering with Southeast University, Nanjing, China. His research interests include electrical system design, rehabilitation engineering, and digital signal processing.

HONGXING WANG was born in Shandong Province, China. He received the master's degree in rehabilitation medicine and the Ph.D. degree in rehabilitation medicine from Nanjing Medical University, Nanjing, China, in 2003 and 2015, respectively.

From August 2003 to May 2019, he worked at the Department of Rehabilitation Medicine, 1st Affiliated Hospital, Nanjing Medical University, Nanjing, China. Since June 2019, he has been a Full Professor and the Director of the Department of Rehabilitation Medicine, Zhongda Hospital, Southeast University, Nanjing China. From October 2012 to November 2013, he also worked as a Research Scholar on neural repair and recovery of spinal cord injury at the Stark Neuroscience Institute of Indiana University, Indianapolis, IN, USA. His studies have focused on clinical neurorehabilitation and functional assessment as well as basic research on stroke and spinal cord injury. Furthermore, he specializes in electromyography diagnosis and electrophysiological evaluation of central and peripheral nervous system disorders.

BILEI WANG received the B.S. degree in clinical medicine and the M.S. and Ph.D. degrees in internal medicine from the Nantong University Medical School, Nantong, China, in 2003, 2006, and 2018, respectively.

She has been working with the Zhongda Hospital, Southeast University, since 2006, engaged in clinical work on rehabilitation medicine. She specializes in the comprehensive treatment of hemiplegia, swallowing, and speech cognitive impairment after brain injury, and rehabilitation after spinal cord injury and spasm.

XIAOYING LÜ was born in Shanghai, China. She received the M.Med. degree from Shanghai Second Medical University, in 1986, and the Dr.-Dent. degree from Freiburg University, Freiburg, Germany, in 1996.

From 1996 to 1997, she was a Postdoctoral Researcher with Freiburg University. In 1997, she became an Associate Professor at Southeast University, China, and since 2003, she has been a Full Professor.

JIA HUANG was born in Gansu, China. She graduated from the Medical School of Southeast University in 2004, majoring in clinical medicine. She has been working with the Zhongda Hospital, Southeast University, since 2004, engaged in clinical work on rehabilitation medicine. She specializes in the comprehensive treatment of hemiplegia, swallowing, and speech cognitive impairment after brain injury, and rehabilitation after spinal cord injury and spasm.

ZHIGONG WANG (Senior Member, IEEE) was born in Henan, China. He received the M.Eng. degree in radio engineering from the Nanjing Institute of Technology (now Southeast University), Nanjing, China, in 1981, and the Dr.-Ing. degree in electronic engineering from Ruhr-University Bochum, Germany, in 1990.

From 1977 to 1981, he worked on radio communication techniques and computer-aided circuit designs at the Nanjing Institute of Technology. From 1985 to 1990, he worked on high-speed silicon bipolar circuit designs for multigigabit/s fiber-optic communication at Ruhr-University Bochum, Germany. From 1990 to 1997, he was with the Fraunhofer Institute of Applied Solid State Physics, Freiburg, Germany, working on high-speed GaAs ICs for fiber-optic data transmission and MMICs. Since October 1997, he has been a Full Professor with Southeast University, Nanjing, China.

● ● ●